Lasers in Eng., Vol. 46, pp. 359–366
Reprints available directly from the publisher
Photocopying permitted by license only

©2020 Old City Publishing, Inc.
Published by license under the OCP Science imprint,
a member of the Old City Publishing Group

Direct Laser Grain Writing in Steels

D. GORTAT[1,*], M. SPARKES[1], S.B. FAIRCHILD[2] AND W. O'NEILL[1]

[1]*Institute for Manufacturing, University of Cambridge, 17 Charles Babbage Road, Cambridge CB3 0FS, UK*
[2]*Materials and Manufacturing Directorate, Air Force Research Laboratory, Wright-Patterson AFB, OH 45433-0000, USA*

Laser melting the surface of 304 stainless steel allows controlled grain growth in the direction of the laser scan [1]. We demonstrate the application of laser surface melting with a Yb fibre laser as a technique for single crystal grain refinement and security marking in polycrystalline metals *via* localized grain nucleation. Single crystals were achieved after three consecutive passes with constant laser parameters throughout the length of the laser raster at 19.17 kJ/cm^2 average energy at 300K, 0.1% O_2 environment. The depth of localized grain nucleation was measured to be approximately 20 mm for a single pass, making hidden messages in the bulk of the material possible after mechanically removing the immediate surface melt. The patterns are undetectable by conventional optical microscopy but can be viewed with interferometric microscopy due to fine height differences between untreated and laser treated surface regions, this way establishing a metal security marking technique.

Keywords: Yb fibre laser, 304 stainless steel, 316 stainless steel, laser surface melting, microstructure, single crystal, security marking

1 INTRODUCTION

Unbroken continuous grains with no grain boundaries, yield unique properties in the lattice of metals, such as high electrical and thermal conductivity [2] and allow production of high strength low creep parts, applications of which can be found, primarily, in the aircraft industry [3]. They also pose a significant fabrication challenge due to the liquid-solid transformation. The environmental conditions during manufacturing require strict control in order

*Corresponding author: E-mail: dg458@cam.ac.uk

to stabilise the growth of the initially formed nuclei in the liquid phase [4]. The conventional methods of fabrication are the Czochralski process, pulling the crystal from melt against gravity forces [5] and the Bridgeman technique, heating above melting temperature then slow-cooling the seed crystal [6]. In recent years, in additive manufacturing technologies, selective laser melting has been observed to generate single crystal microstructures in steels [7–9].

We demonstrate the application of optimizing the laser surface melting processing parameters including laser power, scanning speed and number of laser passes for single crystal grain refinement in polycrystalline metals. The method was applied to metal laser security marking. Laser engraving is widely used in industry for identification and traceability purposes. The primary concern for such markings is their readability and durability, therefore, deep laser markings 5 to 20 μm are desirable [10]. The grain refined markings can serve as long lasting security identifiers in metal parts. Laser surface melting forms grain patterns in metal's microstructure corresponding to the surface melt, independent of the surface quality. Mechanically removing the immediate surface melt leaves underlying surface patterns undetectable by conventional optical microscopy which can be viewed with differential interference contrast (DIC) microscopy or grain imaging tools such as focused ion beam (FIB) and electron backscatter diffraction (EBSD), this way establishing a metal security marking technique *via* localized laser grain nucleation.

2 EXPERIMENTAL PROCEDURES

A Yb non-polarized fibre laser (G3; SPI Lasers, Ltd.) emitting a Gaussian beam at a wavelength of 1.064 μm, an output beam M^2=2 and maximum output power of 20 W in the continuous wave (CW) mode was used for melting the surface of 3 mm thick 304 stainless steel and 1 mm 316 stainless steel plates. Laser beam focusing was achieved with a lens (03-90FT; Jenoptic AG) of focal length of 125 mm and calculated $1/e^2$ 39.4 μm spot size. The samples were processed at room temperature with a continuous flow of N_2 supplied into the irradiated area to minimize the sample's oxidation. An oxygen meter (GOX 100T; Greisinger, GmbH) was used to track the O_2 levels to 0.1 to 0.2%. Ethanol was used to remove contaminants from the sample's surface prior to laser processing.

For the depth measurements, the stainless steel samples were cut along the laser scanning track and the cross-sectional area was then mechanically polished and chemically etched in stainless steel micro-etchant with a chemical composition 10 g $FeCl_3$ 30 ml HCl 120 ml water at room temperature to reveal the laser penetration depth into the materials. For characterization, an optical microscope (BX51; Olympus, Ltd.) with a camera (ProgRes C10+; Jenoptic AG) was used; along with DIC (BX51M; Olympus, Ltd.). A white light interferometer (WLI) (NT3300; Veeco Instruments, Inc.) was used for surface

roughness measurements. For microstructural imaging a FIB (Helios NanoLab 650; FEI Corporation) was utilized without surface preparation. The FIB grain orientation contrast is caused by the depth of penetration of the channelled incident ions, which varies with the relative angle between the ion beam and the lattice plane and the interplanar spacing of the lattice [11]. For characterizing the grain diameter a scanning electron microscope (SEM) (Helios NanoLab 650; FEI Corporation) with EBSD analysis capability was used.

3 RESULTS AND DISCUSSION

The average grain diameter in 304 stainless steel and 316 stainless steel was measured to be 10.72 and 9.10 μm, respectively, ensuring the processing laser spot of 39.4 μm covers each individual grain. The 304 stainless steel was irradiated normal to the laser beam in three consecutive laser passes with a constant laser energy density) of 19.17 kJ/cm^2, scanning speed of 2.25 mm/s, to increase the localized grain nucleation volume in sample's microstructure. A single laser pass with 19.17 kJ/cm^2 energy density produced a meltpool approximately 20 mm deep in both 304 stainless steel and 316 stainless steel.

Figure 1 shows a cross-section view of the surface laser meltpool in the 304 stainless steel and 316 stainless steel samples where the treated region is comprised of a laser surface melted zone (LSMZ) and heat affected zone (HAZ). The SEM images in Figure 2 show the surface structure and the FIB images of the underlying microstructure of the 304 stainless steel before and after laser irradiation. Upon second laser pass in the same area, keeping laser parameters constant, the grains in the middle of the pass increase in size to 29.17 μm diameter and develop an ordered structure in the scan direction, as can be seen from Figure 3. With the third laser pass the grains are stretched into long single crystals across the width of the laser pass, 295 μm long, 94.41 μm in diameter, as shown in Figure 4.

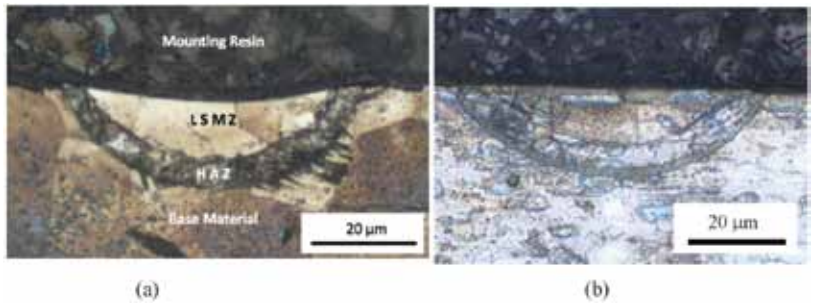

FIGURE 1
Optical cross-sectional micrographs of (a) a single pass scanned 304 stainless steel and (b) 316 stainless steel with average laser energy density of 19.17 kJ/cm^2.

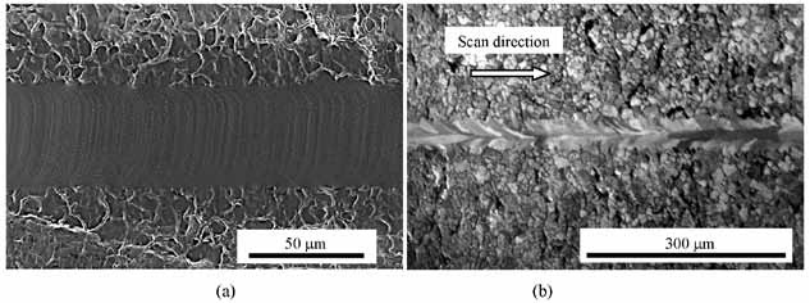

FIGURE 2
(a) SEM and (b) FIB images of the 304 stainless steel irradiated with 19.17 kJ/cm^2 laser intensity, single pass.

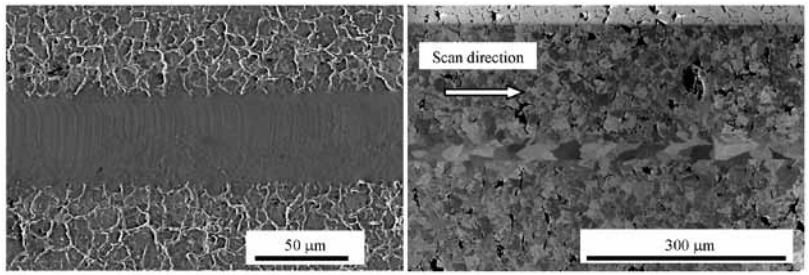

FIGURE 3
(a) SEM and (b) FIB images of the 304 stainless steel irradiated with 19.17 kJ/cm^2 laser intensity, double pass.

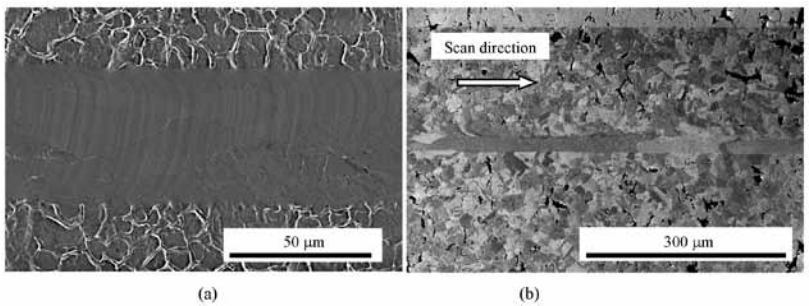

FIGURE 4
(a) SEM and (b) FIB images of the 304 stainless steel irradiated with 19.17 kJ/cm^2 laser intensity, triple pass.

The surface experiences a ripple effect due to the surface tension [12] response to high levels of energy density. Subsequent remelting increases the laser pass width due to increased photon coupling in the laser polished area caused by surface roughness decrease, as is evident from Figure 5.

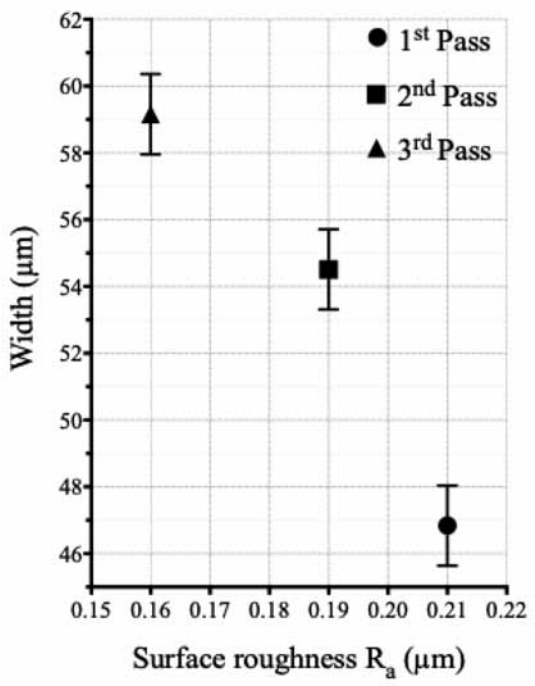

FIGURE 5
Surface roughness measurements *versus* laser pass width for the 304 stainless steel samples for single crystal growth.

The sample exhibits a surface morphology difference between the treated and untreated surface areas on microscale due to the grain size difference. This is attributed to the sample now having different surface strength in its treated and untreated regions [13]. Because of this, applying plastic deformation uniformly across its surface *via* mechanical polishing creates fine height differences between the microstructurally refined regions of the sample, detectable by the interferometric techniques.

Due to the single laser pass already producing 20 µm meltpools and not to undermine the pattern's precision, as was discovered with multiple laser passes, laser surface melting for metal security marking was implemented *via* single scan patterning.

Letters and numbers were laser melted in the surface of steel samples with the above parameters. The irradiated stainless steel samples were then mechanically polished from original roughness of R_a=280 ±1.20 µm to the surface roughness of R_a=12.06 ±0.73 nm to ensure the complete removal of the immediate surface melt. Optical microscopy showed little evidence of visible melt pools, as can be seen from Figure 6(a). The patterns were clearly visible, however, with the DIC microscopy, as can be seen from Figure 6(b),

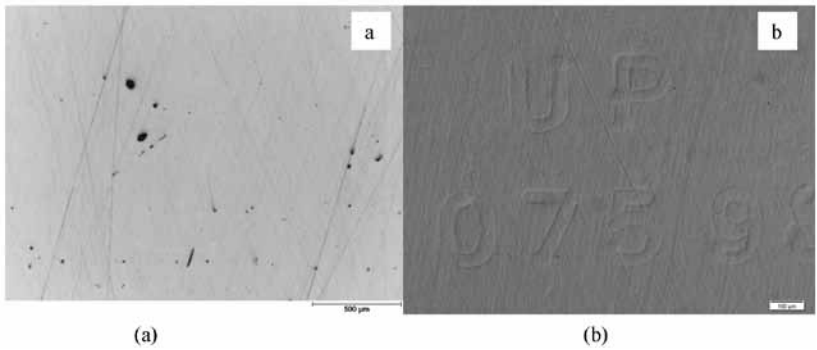

FIGURE 6
(a) Optical microscope image showing the surface of 316 stainless steel after laser irradiation and mechanical polishing, and (b) optical image with a Nomarski microscope showing the 316 stainless steel surface where letters and numbers are visible.

due to the light rays reflecting simultaneously from treated and untreated regions on the sample, highlighting the morphological difference between them. WLI showed the maximum R_t value of the surface height discrepancy to be around 40 nm, Figure 7.

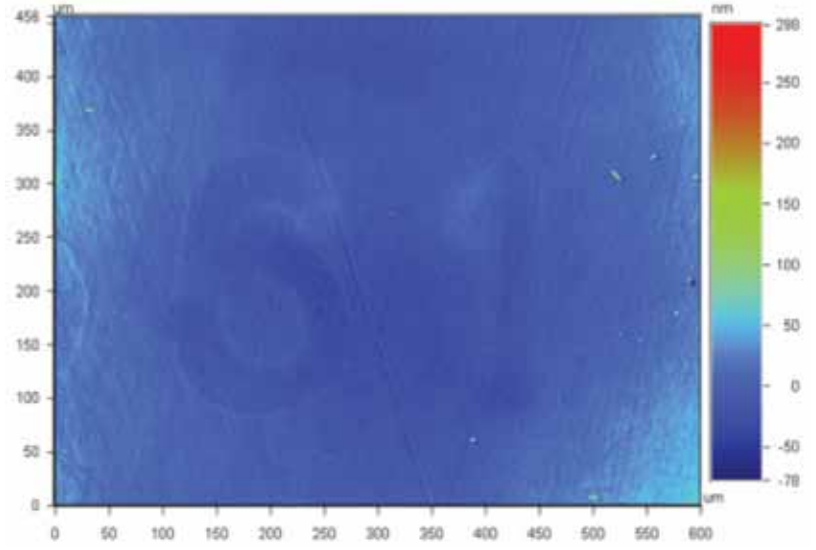

FIGURE 7
Interferometer micrograph of the laser inscribed 316 stainless steel surface with numbers 61 after the mechanical polishing. Maximum peak to valley difference is approximately 40 nm.

4 CONCLUSIONS

Multiple passes over the surface of 304 stainless steel and 316 stainless steel with a Yb fibre laser beam were observed to generate single crystals within the irradiated area with no added gasses or sample pre-heating. A grain enlargement after three consecutive passes with constant laser parameters throughout the length of the laser raster was observed when the laser parameters were kept constant at 19.17 kJ/cm^2 average energy density at 300 K, 0.1% O_2 environment. By controlling the direction and area of laser irradiation the laser surface melting method made possible to directly draw with grains in the microstructure of 304 stainless steel and 316 stainless steel. Removing the surface melt *via* mechanical polishing allows to hide the patterns from optical light microscopy establishing this way a metal security marking technique. The hidden patterns can be viewed with interferometric microscopy due to fine height difference between the untreated and treated areas in sample's microstructure. The viewing contrast is dependent on the grain size and, therefore, can be further increased *via* multiple laser passes.

REFERENCES

[1] Gortat D., Sparkes M., Fairchild S.B., Murray P.T., Cahay M.M., Back T.C., Gruen G.J., Lockwood N.P. and O'Neill W. Laser surface melting of stainless steel anodes for reduced hydrogen outgassing. *Materials Letters* **190** (2017), 5-8.

[2] Prajapati A.and Rajpurohit S. Formation and applications of single crystal material. *Indian Journal of Scientific Research* **17**(2) (2017), 53-59.

[3] Gell M., Duhl D. and Giamei A. F. The development of single crystal superalloy turbine blades. *Superalloys* **21** (1980), 205-214.

[4] Feigelson R. *50 Years Progress in Crystal Growth: A Reprint Collection*. New York: Elsevier. 2004.

[5] Pajączkowska A. Jan Czochralski and his method of crystal growth. *Acta Physica Polonica A* **124**(2) (2013), 171-172.

[6] Bridgman P.W. Certain physical properties of single crystals of tungsten, antimony, bismuth, tellurium, cadmium, zinc, and tin. *Proceedings of the American Academy of Arts and Sciences* **60**(6) (1925), 305-383.

[7] Chen J., Schwarze D. and Niendorf T. Single crystal microstructure built by selective laser melting. Lasers in Manufaturing (LiM 2017). 26-29 June 2017, Munich, Germany.

[8] Niendorf T., Leuders S., Riemer A., Richard H., Tröster T. and Schwarze D. Highly anisotropic steel processed by selective laser melting. *Metallurgical and Materials Transactions B: Process Metalluergy and Materials Processing Science* **44**(4) (2013), 794-796.

[9] Carter L.N., Martin C., Withers P.J. and Attallah M.M. The influence of the laser scan strategy on grain structure and cracking behaviour in SLM powder-bed fabricated nickel superalloy. *Journal of Alloys and Compounds* **615** (2014), 338-347.

[10] Lam Y.C., Zheng H.Y., Tjeung R.T. and Chen X. Seeing the invisible laser markings. *Journal of Physics D: Applied Physics* **42**(4) (2009), 042004.

[11] Phaneuf M.W. Applications of focused ion beam microscopy to materials science specimens. *Micron* **30**(3) (1999), 277-288.

[12] Temmler A., Willenborg E. and Wissenbach K. Laser polishing. *Proceedings of the SPIE: Laser Applications in Microelectronic and Optoelectronic Manufacturing (LAMOM) XVII* **82430** (2012), 82430W-13.

[13] Zhang X., Hansen N., Gao Y. and Huang X. Hall–Petch and dislocation strengthening in graded nanostructured steel. *Acta Materialia* **60**(16) (2012), 5933-5943.